We are IntechOpen, the world's leading publisher of Open Access books Built by scientists, for scientists

4,800
Open access books available

122,000
International authors and editors

135M
Downloads

Our authors are among the

154
Countries delivered to

TOP 1%
most cited scientists

12.2%
Contributors from top 500 universities

CLARIVATE ANALYTICS BOOK CITATION INDEX INDEXED

WEB OF SCIENCE™

Selection of our books indexed in the Book Citation Index in Web of Science™ Core Collection (BKCI)

Interested in publishing with us?
Contact book.department@intechopen.com

Numbers displayed above are based on latest data collected.
For more information visit www.intechopen.com

3

Quaternary Volcanism Along the Volcanic Front in Northeast Japan

Koji Umeda[1] and Masao Ban[2]
[1]*Geological Isolation Research and Development Directorate, Japan Atomic Energy Agency*
[2]*Department of Earth and Environmental Sciences, Yamagata University*
Japan

1. Introduction

Northeast Japan parallels a subduction zone where the Pacific plate converges against the North American plate. The axial part of Northeast Japan is composed of an uplifted mountain range called the Ou Backbone Range, along which a number of Quaternary volcanoes are distributed. The eastern margin of these volcanoes defines part of the Quaternary volcanic front of Northeast Japan (Fig. 1). The chemical composition of the volcanic rocks indicates a strong across variation in the alkali content and other incompatible elements, which are lower along the volcanic front and gradually increase rearward (Nakagawa et al., 1988; Yoshida, 2001). The Sr isotope compositions also indicate across-arc variation; the fore-arc volcanoes have higher $^{87}Sr/^{86}Sr$ ratios (0.704-0.705) than the rear-arc volcanoes (around 0.703) (Notsu, 1983; Kumura & Yoshida, 2006). Such variations can be ascribed to heterogeneous subcontinental lithosphere and/or additional of components from the subducted slab (e.g., Sakuyama & Nesbitt, 1986; Tatsumi & Eggins, 1995). This trench-parallel chemical zonation in Northeast Japan has been established since ca. 12 Ma (Yoshida, 2001).

The late Miocene to Quaternary evolution of the volcanic arc of Northeast Japan has been accompanied by some remarkable features. These include (1) Late Miocene to Pliocene caldera-forming volcanism phase, under a direction of maximum compression oblique to the arc and (2) Quaternary andesite stratovolcano-forming volcanism phase, under orthogonal convergence settings (Acocella et al., 2008). A compressive stress regime under orthogonal convergence is unfavourable to facilitate caldera-forming volcanism requiring the formation of a large magma reservoir at shallow depth (Yoshida, 2001). The predominance of stratovolcanoes is reconciled with compressional tectonic settings in the present-day subduction system. Nevertheless, it remains obscure as to when the andesite stratovolcano-forming volcanism has been established under Quaternary orthogonal convergence in Northeast Japan.

In general, characteristics of volcanism such as distribution of volcanoes, type of eruptions, magma discharge rate are closely associated with tectonics surrounding the volcanoes. It is very important to examine the relationship between them for better understanding magmatism in various tectonic settings. In this chapter, the temporal changes in the distribution, type and magma discharge rate of the volcanoes near the volcanic front (i.e., Nasu Volcanic Zone) during the last 2.0 m. y. were clarified based on the age and volume

data of the Quaternary volcanoes in Northeast Japan presented by Martin et al. (2004). In addition, we examine the relationship between variations in Quaternary volcanism and tectonics specifically with regard to faulting and uplifting.

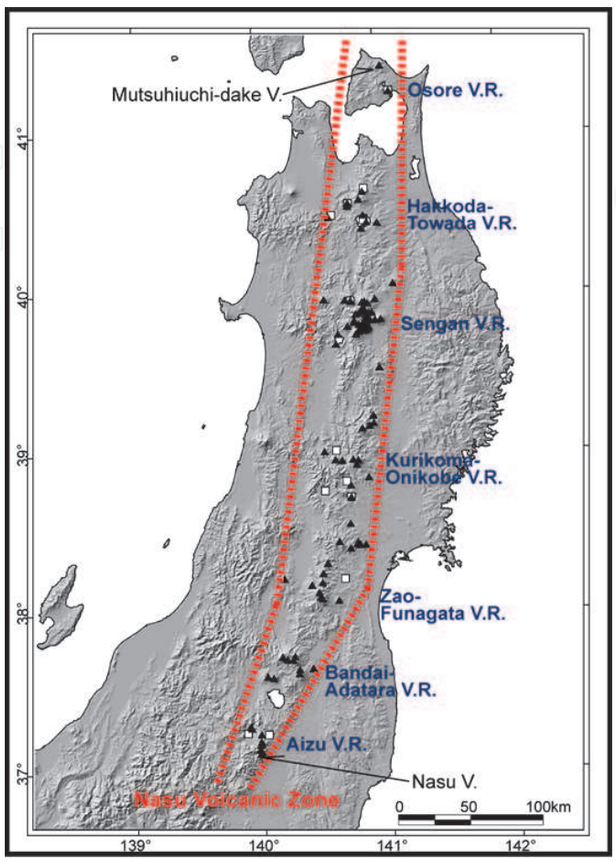

Fig. 1. Distribution of volcanic centers in Northeast Japan since 2.0 Ma. Solid triangle and open square represent stratovolcano and large-scale caldera volcanoes, respectively.

2. Volcanism during the last 2.0 million years

Thirty four Quaternary volcanoes have been recognized along the volcanic front between Mutsuhiuchi-dake volcano and Nasu volcano (Ono et al., 1981), and their eruptive volumes were calculated (Aramaki & Ui 1978). To refine the sequence of volcanism during the last 2.0 million years, Umeda et al. (1999) subdivided individual volcanoes into as small a unit as possible, and estimated their active periods from radioactive age and stratigraphic data, and calculated their eruptive volumes. Recently, Martin et al. (2004) revised the database of Umeda et al. (1999) using the "Catalog of Quaternary volcanoes in Japan" of Committee for Catalogue of Quaternary Volcanoes in Japan eds. (1999) and other new radiometric age data for each volcano along the volcanic front in Northeast Japan. Martin et al. (2004) refers to "Volcanic Event" that is defined as multiple eruptions from the same conduit occurring over several tens to hundreds of thousands of years (Table 1). By defining the highest points of the individual stratovolcanoes or the geometrical centers of the calderas as volcanic centers (the main vents) for each volcanic event, the locations, magma volume and eruption styles were evaluated to clarify the temporal change in volcanism.

Volcano Complex	Volcanic event	Location		Age (Ma)			Volume
		Latitude	Longitude	Oldest	Approxi-mate	Younge-st	(km³, DRE)
Mutsuhiuchi-dake	Older Mutsuhiuchi-dake	41.437	141.057		ca.0.73		5.9
Mutsuhiuchi-dake	Younger Mutsuhiuchi-dake	41.437	141.057	0.45		0.2	3.6
Osorezan	Kamabuse-yama	41.277	141.123		ca.0.8		11.4
Hakkoda	Hakkoda P.F.1st.	40.667	140.897		0.65		17.8
Hakkoda	South-Hakkoda	40.600	140.850	0.65	—	0.4	52.4
Hakkoda	Hakkoda P.F.2nd.	40.667	140.897		0.4		17.3
Hakkoda	North-Hakkoda	40.650	140.883	0.16	—	0	30.4
Okiura	Aoni F. Aonigawa P.F.	40.573	140.763		ca.1.7		17.6
Okiura	Aoni F. Other P.F.	40.573	140.763	1.7	—	0.9	3.7
Okiura	Okogawasawa lava	40.579	140.759	0.9	-	0.65	0.9
Okiura	Okiura dacite	40.557	140.755	0.9	-	0.7	2.1
Ikarigaseki	Nijikai Tuff	40.500	140.625		ca.2.0		20.2
Ikarigaseki	Ajarayama	40.490	140.600	1.91	—	1.89	2.1
Towada	Herai-dake	40.450	141.000				5.1
Towada	Ohanabe-yama	40.500	140.883	0.4	—	0.05	8.9
Towada	Hakka	40.417	140.867				1.4
Towada	Towada Okuse	40.468	140.888		0.055		4.8
Towada	Towada Ofudo	40.468	140.888		0.025		22.1
Towada	Towada Hachinohe	40.468	140.888		0.013		26.9
Towada	Post-caldera cones	40.457	140.913	0.013	—	0	14.4
Nanashigure	Nanashigure	40.068	141.112	1.06	—	0.72	55.5
Moriyoshi	Moriyoshi	39.973	140.547	1.07	—	0.78	18.1
Bunamori	Bunamori	39.967	140.717		1.2		0.1
Akita-Yakeyama	Akita-Yakeyama	39.963	140.763	0.5	—	0	9.9
Nishimori/ Maemori	NIshimori/Maemori	39.973	140.962	0.5	—	0.3	2.6
Hachimantai/ Chausu	Hachimantai	39.953	140.857	1	—	0.7	5.5
Hachimantai/ Chausu	Chausu-dake	39.948	140.902	0.85	—	0.75	13.7
Hachimantai/ Chausu	Fukenoyu	39.953	140.857		ca.0.7		0.2
Hachimantai/ Chausu	Gentamri	39.956	140.878				0.2
Yasemori/ Magarisaki-yama	Magarisaki-yama	39.878	140.803	1.9	—	1.52	0.3
Yasemori/ Magarisaki-yama	Yasemori	39.883	140.828		1.8		0.9
Kensomori/ Morobidake	Kensomori	39.897	140.871		ca.0.8		0.8
Kensomori/ Morobidake	Morobi-dake	39.919	140.862	1	—	0.8	2.5

Volcano Complex	Volcanic event	Location		Age (Ma)			Volume
		Latitude	Longitude	Oldest	Approxi-mate	Younge-st	(km^3, DRE)
Kensomori/ Morobidake	1470m Mt. lava	39.909	140.872				0.1
Kensomori/ Morobidake	Mokko-dake	39.953	140.857		ca.1.0		0.5
Tamagawa Welded Tuff	Tamagawa Welded Tuffs R4	39.963	140.763		ca.2.0		83.2
Tamagawa Welded Tuff	Tamagawa Welded Tuffs D	39.963	140.763		ca.1.0		32.0
Nakakura/ Shimokura	Obuka-dake	39.878	140.883	0.8	—	0.7	2.9
Nakakura/ Shimokura	Shimokura-yama	39.889	140.933				0.4
Nakakura/ Shimokura	Nakakura-yama	39.888	140.910				0.4
Matsukawa	Matsukawa andesite	39.850	140.900	2.6	—	1.29	11.6
Iwate/ Amihari	Iwate	39.847	141.004	0.2	—	0	25.1
Iwate/ Amihari	Amihari	39.842	140.958	0.3	—	0.1	10.6
Iwate/ Amihari	Omatsukura-yama	39.841	140.919	0.7	—	0.6	3.3
Iwate/ Amihari	Kurikigahara	39.849	140.882				0.2
Iwate/ Amihari	Mitsuishi-yama	39.848	140.900		0.46		0.6
Shizukuishi/ Takakura	Marumori	39.775	140.877	0.4	—	0.3	2.4
Shizukuishi/ Takakura	Shizukuishi-Takakura-yama	39.783	140.893	0.5	—	0.4	5.2
Shizukuishi/ Takakura	Older Kotakakura-yama	39.800	140.900		1.4		2.7
Shizukuishi/ Takakura	North Mikado-yama	39.800	140.875				0.3
Shizukuishi/ Takakura	Kotakakura-yama	39.797	140.907	0.6	—	0.5	1.8
Shizukuishi/ Takakura	Mikado-yama	39.788	140.870		ca.0.3		0.2
Shizukuishi/ Takakura	Tairagakura-yama	39.808	140.878		ca.0.3		0.1
Nyuto/ Zarumori	Tashirotai	39.812	140.827	0.3	—	0.2	0.6
Nyuto/ Zarumori	Sasamori-yama	39.770	140.820	0.23	—	0.1	0.4
Nyuto/ Zarumori	Yunomori-yama	39.772	140.827		ca.0.3		0.5
Nyuto/ Zarumori	Zarumori-yama	39.788	140.850		0.56		0.9
Nyuto/ Zarumori	Nyutozan	39.802	140.843	0.58	—	0.5	5.0

Volcano Complex	Volcanic event	Location		Age (Ma)			Volume
		Latitude	Longitude	Oldest	Approxi-mate	Younge-st	(km³, DRE)
Nyuto/ Zarumori	Nyuto-kita	39.817	140.855		ca.0.4		0.1
Akita-Komagatake	Akita-Komagatake	39.754	140.802	0.1	—	0	2.9
Kayo	Kayo	39.803	140.735	2.2	—	1.17	5.9
Kayo	KoJiromori	39.828	140.787		0.94		0.3
Kayo	Akita-Ojiromori	39.839	140.788	1.7	1.7	1.7	0.3
Innai/ Takahachi	Takahachi-yama	39.755	140.655	1.7	1.7	1.7	0.0
Innai/ Takahachi	Innai	39.692	140.638	2	—	1.6	0.5
Kuzumaru	Aonokimori andesites	39.543	140.983		2.06		0.3
Yakeishi	Yakeishidake	39.161	140.832	0.7	—	0.6	9.5
Yakeishi	Komagatake	39.193	140.924		ca.1.0		7.6
Yakeishi	Kyozukayama	39.178	140.892	0.6	—	0.4	5.7
Yakeishi	Usagimoriyama	39.239	140.924	0.07	—	0.04	2.3
Kobinai	Kobinai	39.018	140.523	1	—	0.57	2.3
Takamatsu/ Kabutoyama	Kabutoyama Welded Tuff	39.025	140.618		1.16		3.2
Takamatsu/ Kabutoyama	Kiji-yama Welded Tuffs	39.025	140.618		0.30		5.1
Takamatsu	Takamatsu	38.965	140.610	0.3	—	0.27	3.8
Takamatsu	Futsutsuki-dake	38.961	140.661		ca.0.3		0.8
Kurikoma	Tsurugi-dake	38.963	140.792	0.1	—	0	0.2
Kurikoma	Magusa-dake	38.968	140.751	0.32	—	0.1	1.5
Kurikoma	Kurikoma	38.963	140.792	0.4	—	0.1	0.9
Kurikoma	South volcanoes	38.852	140.875		ca.0.5		0.3
Kurikoma	Older Higashi Kurikoma	38.934	140.779		ca.0.5		2.2
Kurikoma	Younger Higashi Kurikoma	38.934	140.779	0.4	—	0.1	0.7
Mukaimachi	Mukaimachi	38.770	140.520		ca.0.8		12.0
Onikobe	Shimoyamasato tuff	38.830	140.695	0.21	0.21	0.21	1.0
Onikobe	Onikobe Centeral cones	38.805	140.727		ca.0.2		1.1
Onikobe	Ikezuki tuff	38.830	140.695	0.3	—	0.2	17.3
Naruko	Naruko Central cones	38.730	140.727		ca.0.045		0.1
Naruko	Yanagizawa tuff	38.730	140.727		ca.0.045		4.8
Naruko	Nizaka tuff	38.730	140.727		ca.0.073		4.8
Funagata	Izumigatake	38.408	140.712	1.45	—	1.14	2.3
Funagata	Funagatayama	38.453	140.623	0.85	—	0.56	19.0
Yakuraisan	Yakuraisan	38.563	140.717	1.65	—	1.04	0.2
Nanatsumori	Nanatsumori lava	38.430	140.835	2.3	—	2	0.5
Nanatsumori	Miyatoko Tuffs	38.428	140.793		ca.2.5		6.1
Nanatsumori	Akakuzure-yama lava	38.433	140.768	1.6	—	1.5	1.5
Nanatsumori	Kamikadajin lava	38.447	140.772	1.6	—	1.5	0.8
Shirataka	Shirataka	38.220	140.177	1	—	0.8	3.8

Volcano Complex	Volcanic event	Location		Age (Ma)			Volume
		Latitude	Longitude	Oldest	Approxi-mate	Younge-st	(km^3, DRE)
Adachi	Adachi	38.218	140.662		ca.0.08		0.9
Gantosan	Gantosan	38.195	140.480	0.4	—	0.3	4.6
Kamuro-dake	Kamuro-dake	38.253	140.488		ca.1.67		5.7
Daito-dake	Daito-dake	38.316	140.527				5.7
Ryuzan	Ryuzan	38.181	140.397	1.1	—	0.9	4.6
Zao	Central Zao 1st.	38.133	140.453	1.46	—	0.79	0.8
Zao	Central Zao 2nd.	38.133	140.453	0.32	—	0.12	15.2
Zao	Central Zao 3rd.	38.133	140.453	0.03	—	0	0.0
Zao	Sugigamine	38.103	140.462		1		9.9
Zao	Fubosan/byobudake	38.093	140.478	0.31	—	0.17	15.2
Aoso-yama	Gairinzan	38.082	140.610	0.7	—	0.4	6.1
Aoso-yama	Central Cone	38.082	140.610	0.4	—	0.38	3.0
Azuma	Azuma Kitei lava	37.733	140.247	1.3	—	1	24.7
Azuma	Higashi Azumasan	37.710	140.233	0.7	—	0	22.8
Azuma	Nishi Azumasan	37.730	140.150	0.6	—	0.4	7.2
Azuma	Naka Azumasan	37.713	140.188	0.4	—	0.3	4.6
Nishikarasu-gawa andesite	Nishikarasugawa andesite	37.650	140.283		ca.1.5		1.9
Adatara	Adatara Stage 1	37.625	140.280	0.55	—	0.44	0.3
Adatara	Adatara Stage 2	37.625	140.280		ca.0.35		0.4
Adatara	Adatara Stage 3a	37.625	140.280		ca.0.20		2.0
Adatara	Adatara Stage 3b	37.625	140.280	0.12	—	0.0024	0.3
Sasamori-yama	Sasamari-yama andesite	37.655	140.391	2.5	—	2	0.4
Bandai	Pre-Bandai	37.598	140.075		ca.0.7		0.1
Bandai	Bandai	37.598	140.075	0.3	—	0	14.0
Nekoma	Old Nekoma	37.608	140.030	1	—	0.7	11.4
Nekoma	New Nekoma	37.608	140.030	0.5	—	0.4	0.9
Kasshi/ Oshiromori	Kasshi	37.184	139.973				0.1
Kasshi/ Oshiromori	Oshiromori	37.199	139.970				0.7
Kasshi/ Oshiromori	Matami-yama	37.292	139.886				0.3
Kasshi/ Oshiromori	Naka-yama	37.282	139.899				0.0
Shirakawa	Kumado P.F.	37.242	140.032		1.31		19.2
Shirakawa	Tokaichi A.F. tuffs	37.242	140.032	1.31	—	1.24	12.0
Shirakawa	Ashino P.F.	37.242	140.032		1.2		19.2
Shirakawa	Nn3 P.F.	37.242	140.032	1.2	—	1.17	0.0
Shirakawa	Kinshoji A.F. tuffs	37.242	140.032	1.2	—	1.18	9.0
Shirakawa	Nishigo P.F.	37.252	139.869		1.11		28.8
Shirakawa	Tenei P.F.	37.242	140.032		1.06		7.7
Nasu	Futamata-yama	37.244	139.971		0.14		3.2

Volcano Complex	Volcanic event	Location		Age (Ma)			Volume
		Latitude	Longitude	Oldest	Approxi-mate	Younge-st	(km³, DRE)
Nasu	Kasshiasahi-dake	37.177	139.963	0.6	—	0.4	12.3
Nasu	Sanbonyari-dake	37.147	139.965	0.4	—	0.25	5.5
Nasu	Minami-gassan	37.123	139.967	0.2	—	0.05	8.7
Nasu	Asahi-dake	37.134	139.971	0.2	—	0.05	4.6
Nasu	Chausu-dake	37.122	139.966	0.04	—	0	0.3
Hakkoda	South-Hakkoda	41.437	141.057		ca.0.73		5.9
Hakkoda	Hakkoda P.F.2nd.	41.437	141.057	0.45		0.2	3.6
Hakkoda	North-Hakkoda	41.277	141.123		ca.0.8		11.4
Okiura	Aoni F. Aonigawa P.F.	40.667	140.897		0.65		17.8
Okiura	Aoni F. Other P.F.	40.600	140.850	0.65	—	0.4	52.4
Okiura	Okogawa-sawa lava	40.667	140.897		0.4		17.3
Okiura	Okiura dacite	40.650	140.883	0.16	—	0	30.4
Ikarigaseki	Nijikai Tuff	40.573	140.763		ca.1.7		17.6
Ikarigaseki	Ajarayama	40.573	140.763	1.7	—	0.9	3.7
Towada	Herai-dake	40.579	140.759	0.9	-	0.65	0.9
Towada	Ohanabe-yama	40.557	140.755	0.9	-	0.7	2.1
Towada	Hakka	40.500	140.625		ca.2.0		20.2
Towada	Towada Okuse	40.490	140.600	1.91	—	1.89	2.1
Towada	Towada Ofudo	40.450	141.000				5.1
Towada	Towada Hachinohe	40.500	140.883	0.4	—	0.05	8.9
Towada	Post-caldera cones	40.417	140.867				1.4
Nanashigure	Nanashi-gure	40.468	140.888		0.055		4.8
Moriyoshi	Moriyoshi	40.468	140.888		0.025		22.1
Bunamori	Bunamori	40.468	140.888		0.013		26.9
Akita-Yakeyama	Akita-Yakeyama	40.457	140.913	0.013	—	0	14.4
Nishimori/ Maemori	NIshimori/Maemori	40.068	141.112	1.06	—	0.72	55.5
Hachimantai/ Chausu	Hachimantai	39.973	140.547	1.07	—	0.78	18.1
Hachimantai/ Chausu	Chausu-dake	39.967	140.717		1.2		0.1
Hachimantai/ Chausu	Fukenoyu	39.963	140.763	0.5	—	0	9.9
Hachimantai/ Chausu	Gentamri	39.973	140.962	0.5	—	0.3	2.6
Yasemori/ Magarisaki-yama	Magarisaki-yama	39.953	140.857	1	—	0.7	5.5

Table 1. List of volcanoes along the volcanic front in Northeast Japan (after Martin et al., 2004)

2.1 Number of volcanoes and volcanic regions

The volcanoes are clustered near the volcanic front. Seven volcanic regions (V.R.) can be identified as along the arc and named named as follow: the Osore V.R., the Hakkoda-Towada V.R., the Sengan V.R., the Kurikoma-Onikobe V.R., Zao-Funagata V.R., the Bandai-

Adatara V.R. and the Aizu V.R. Each volcanic region is consists of a number of small- to medium-sized stratovolcanoes, typically measuring less than 10 km^3 in magmatic eruption (DRE). This feature of volcano clustering was first pointed out by Umeda et al. (1999) and re-pointed out by Tamura et al. (2002). However, several volcanic centers have produced large-sized stratovolcanoes or large-scale felsic pyroclastic flows, attaining as much as tens of cubic kilometers in DRE volume. Along the volcanic front in Northeast Japan, 139 volcanic events are recognized (Fig. 1). 113 are stratovolcano-forming events, and the rest are caldera-forming.

2.2 Temporal change in magma discharge rate and eruption style

In order to elucidate temporal variations in the long-term magma discharge rate all over the NE Japan arc, the magma volume erupted every 100 kilo years (long-term discharge rate of magma) was calculated for each volcano during the last 2.0 million years In the case of South-Hakkoda eruptive episode between 0.65 and 0.40 Ma (million years ago) belonging to Hakkoda volcano (Table 1), the erupted volume was estimated to be 52.4 km^3 magma from which 10.5 km^3, 21.0 km^3 and 21.0 km^3 magmas can be allocated to the periods of 0.7 to 0.6 Ma, 0.6 to 0.5 Ma and 0.5 to 0.4 Ma, respectively.

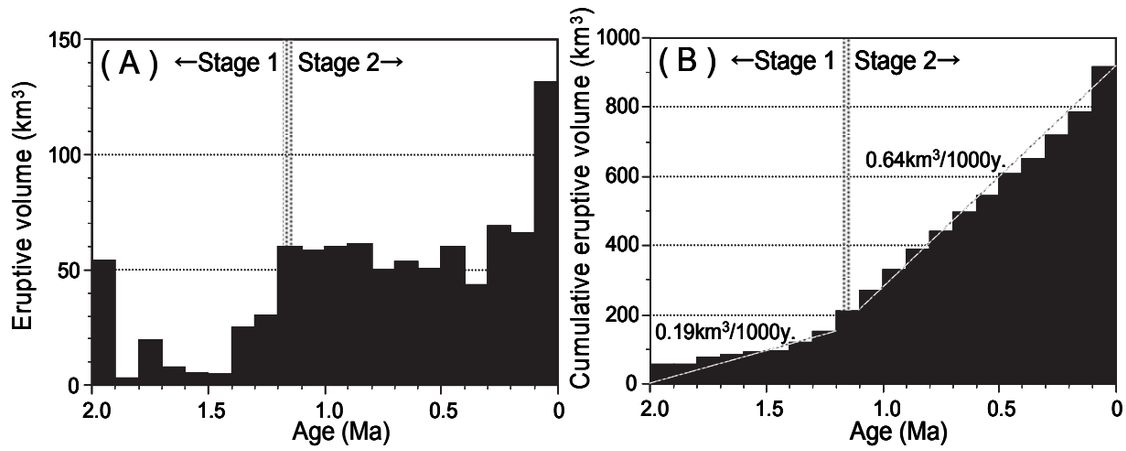

Fig. 2. Temporal changes in eruptive volume (A) and cumulative eruptive volume (B) per 100 ky along the volcanic front in Northeast Japan.

To identify when andesite stratovolcano-forming volcanism was initiated all over the volcanic arc, instead of felsic caldera-forming volcanism, the temporal change in the amount of magma discharged from all the volcanoes is shown in Fig. 2. The figure shows that erupted magma volume increased after 1.2 Ma and more than 50 km^3 of magma per 100,000 years were steadily erupted along the volcanic front.

On the one hand, the temporal change in the amount of erupted magma associated with stratovolcanoes and calderas is shown in Fig. 3. Felsic caldera-forming volcanism with large-scale pyroclastic flows is occurred intermittently since 2.0 Ma, and possible hiatuses of several one hundred thousand years exist during the Quaternary. Andesite stratovolcano-forming volcanism is recognized in the early Quaternary time, and note that it intensified after 1.1 Ma. Thus, Quaternary volcanism along the volcanic front changed in erupted

magma volume and eruption style around 1.2 to 1.1 Ma. It can be characterized in two stages: stage 1 (before ca. 1.2 Ma), dominated by felsic caldera-forming volcanism; stage 2 (ca. 1.2 Ma onwards), was characterized by the predominance of andesite stratovolcano-forming volcanism, and marked by a significant increase in erupted magma volume.

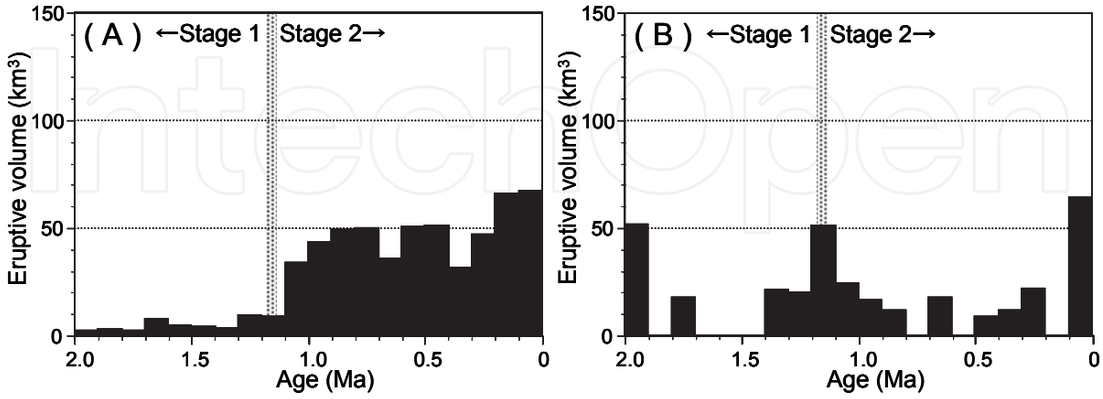

Fig. 3. Temporal changes in eruptive volume for each type of volcanism. (A) is stratovolcano-building volcanism associated with stratovolcanoes, and (B) is felsic caldera-forming volcanism.

2.3 Temporal change in distribution of volcanic centers

The distribution of volcanic centers identified in the two stages discussed above is shown in Fig. 4. Stage 1 volcanism is only recognized in the Hakkoda-Towada V.R., the Sengan V.R., the Zao-Funagata V.R., the Bandai-Adatara V.R. and the Aizu V.R. In contrast, additional volcanic centers in stage 2 emarged in the Osore V.R. and the Kurikoma-Onikobe V.R. in the frontal arc. All seven volcanic regions and the volcanic front in Northeast Japan have only been established since ca.1.2 Ma. Moreover, the distribution of volcanic centers indicates that the northern part of the volcanic front has shifted about 10 to 20 km toward the trench side around 1.2 Ma.

3. Overview of cenozoic tectonism, Northeast Japan

So far, a great deal of effort has been made to obtain information about the Cenozoic tectonism in Northeast Japan (e.g., Sato, 1994; Acocella et al., 2008) and the published results are summarized as follows. The Cenozoic tectonic sequence is directory associated with the separation of the present-day Northeast Japan arc from the Asian continental margin due to the subduction of the Pacific plate and the opening of the Japan Sea rifted. Main rifting started at ~ 23 Ma, and from 21 to 18 Ma, was accompanied by significant counterclockwise rotation of the Northeast Japan arc (Jolivet et al., 1994). Owing to the cessation of the opening of the Japan Sea, the extensional stress field changed at about 13 Ma. In the Middle Miocene to the Pliocene, the tectonics is characterized by very weak crustal deformation under the moderate regional stress field related to the convergence of the Pacific plate (Sato, 1994). The maximum horizontal stress oriented in the NE or ENE direction was manifested during this period. This is one of the reasons why the SW migration of the Kuril sliver due to the oblique convergence along the Kurile arc results from a NE or ENE trending maximum compression (e.g., Otsuki., 1990).

The tectonic shortening became apparent in an E-W direction of compression around the Pliocene to Quaternary boundary, which may be associated with the increase in the motion of the Pacific plate between 5 and 2 Ma (Cox and Engebretson, 1985; Pollitz, 1986). In contrast, the crustal shortening of Northeast Japan might be triggered by the eastward motion of the Amur plate including in the Eurasian plate in the Quaternary (Taira, 2001). This is the reason why the Amur plate is considered to have initiated an incipient subduction on the eastern margin of the Japan Sea (Nakamura, 1983, Tamaki & Honza, 1985). A compressional stress field during the Quaternary is responsible for the development of two narrow uplift zones oriented in the N-S direction, in the Northeast Japan arc: the Ou Backbone Range (fore-arc) and the Dewa Hills (rear-arc). They appear to be an active pop-up structure bounded by opposite-facing reverse faults accommodating < 5 mm/y. of E-W shortening across the range (Hasegawa et al., 2005). Based on the subsurface geology and deformation of river terraces, the initiation time of reverse faulting was estimated at several sites in the Northeast Japan. These results suggest that reverse faulting started in the rear-arc side between 3.4 and 2.4 Ma (Awata and Kakimi, 1985), and in the fore-arc side between 0.9 and 0.5 Ma (Otsuki et al., 1977), corresponding to the onset time of uplift of the Dewa Hills and the Ou Backbone Range. The compressional regime have reactivated normal faults related to the extensional back-arc rifting until 18 Ma as reverse faults and accommodate much of the ongoing shortening across the arc (e.g., Sato, 1994).

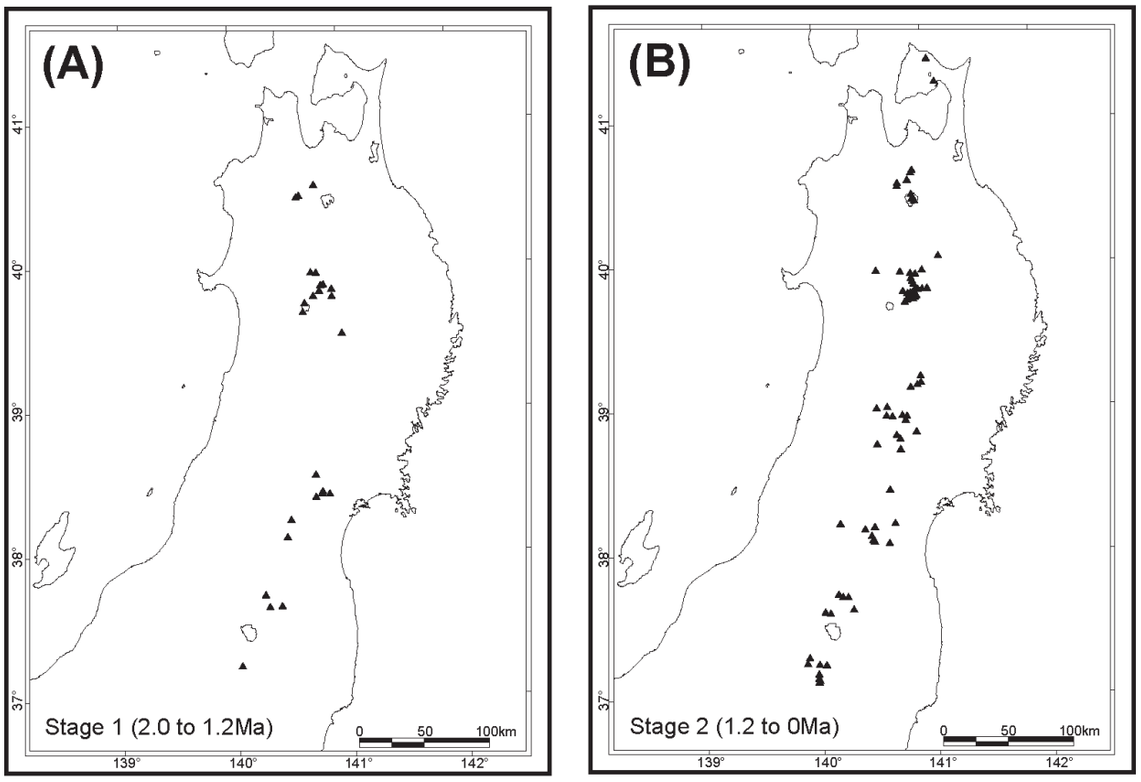

Fig. 4. Distribution of volcanic centers for stage 1 (2.0 –1.2 Ma) and stage 2 (1.2 – 0 Ma).

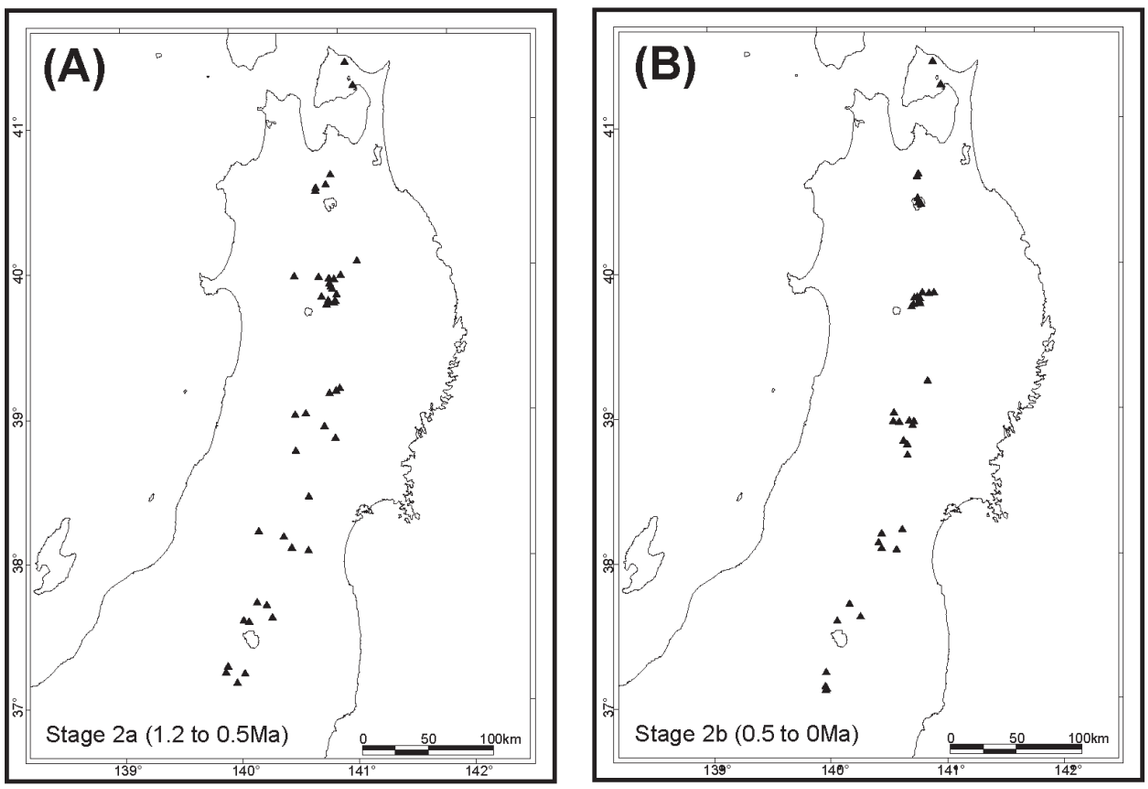

Fig. 5. Distribution of volcanic centers for stage 2a (1.2 –0.5 Ma) and stage 2b (0.5 – 0 Ma).

4. Quaternary volcano-tectonic relationships

Quaternary volcanism and tectonism along the volcanic front are related to each other temporally and spatially. In Northeast Japan, the N-S trending folds and faults have evolved under E-W compression during the Quaternary. Around 1.0 Ma, faulting in the frontal side (Ou Backbone Range), caused the concentrated crustal shortening there. Some contemporaneous changes occurred in volcanism as well; Around 1.2 to 1.1 Ma, felsic caldera-forming volcanism changed to andesite straovolcano-bulding volcanism. Moreover, the total erupted magma volumes along the volcanic front have notably increased since ca. 1.1 Ma. At the same time, magma underwent a systematic change in chemical composition. A significant volume of medium-K andesite has been erupted along the Ou Backbone Range since 1.0 Ma to 0.7 Ma, together with subordinate low-K andesite (Ban et al., 1992). Thus some synchronization between volcanism and tectonism is apparent.

To examine the spatial connections between volcanism and tectonism, the distribution of volcanic centers is compared to those of active faults, amplitudes of uplift and subsidence. Faulting along the volcanic front was initiated around 1.0 Ma and has been intensely activated all over the Ou Backbone Range since 0.5 Ma. The uplift of the mountain range might be accelerated due to resulting in reactivation of more faults. Based on these results, the distribution of volcanic centers along the volcanic front before and after 0.5 Ma, in stage 2, is shown in Fig. 5. The figure indicates that the volcanically active areas became localized near the volcanic front (shifted to the eastern margin of the Ou Backbone Range) after 0.5

Ma, and the alignment of volcanic centers exhibits a weak N-S trend in each volcanic region. Thus, volcanism in stage 2 can be divided into two sub-stages: stage 2a (1.2 to 0.5 Ma), marked by volcanism extended over a wide area and stage 2b (0.5 to 0 Ma), dominated by volcanic centers localized near the volcanic front.

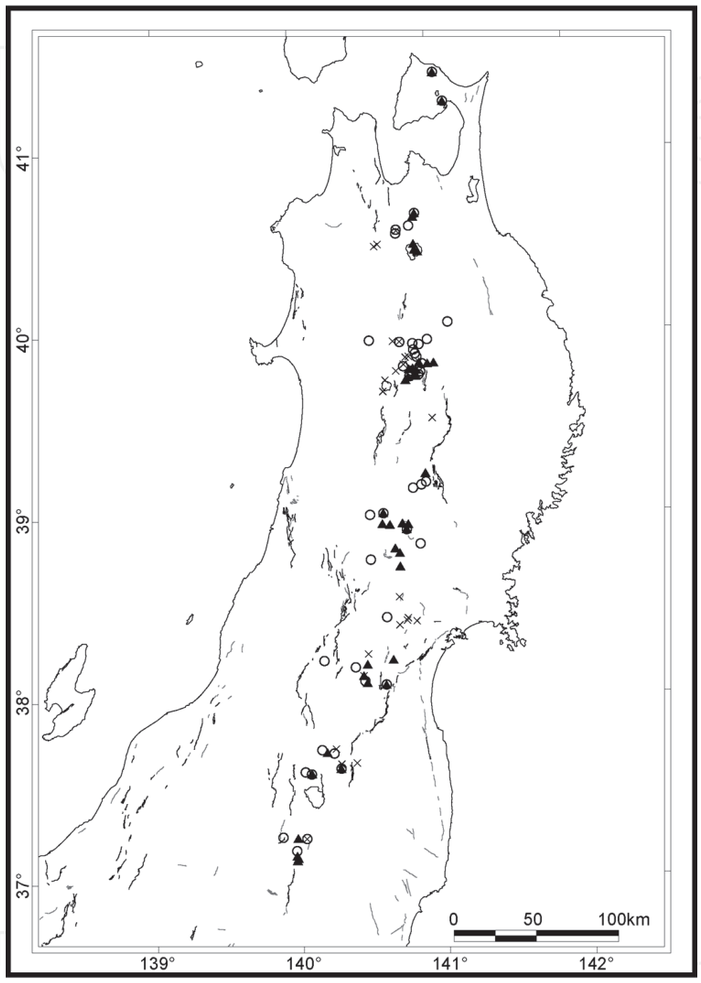

Fig. 6. Distribution of volcanic centers for each stage of Quaternary volcanism (Cross : Stage 1 , Open circle : Stage 2a , Solid triangle : Stage 2b) and active faults.

The distribution of active faults in Northeast Japan (Research Group for Active Faults in Japan, 1991) and volcanic centers formed in the respective stages are shown in Fig. 6. It indicates that the volcanic centers in stage 2b were located in a restricted area between active faults running along the eastern and western margins of the Ou Backbone Range, whereas the volcanic centers in stage 2a are found outside the above area. Fig. 7 shows the uplift and subsidence during the Quaternary (Research Group for Quaternary Tectonic Map, 1968) and the distribution of volcanic centers in the respective stages. Fig. 7 indicates that the volcanic centers formed in stage 2b tend to be distributed more in uplifted areas than those formed in stage 2a. However, there is no active fault near the Hakkoda-Towada V.R. and the Kurikoma-Onikobe V.R., where large-scale felsic pyroclastic flows were

erupted in stage 2b and the amount of uplift is less than in other districts. Thus, the distribution of volcanic centers and eruption styles are closely related to the distribution of active faults and amplitudes of uplift suggesting a spatial connection between volcanism and tectonism (Fig. 8).

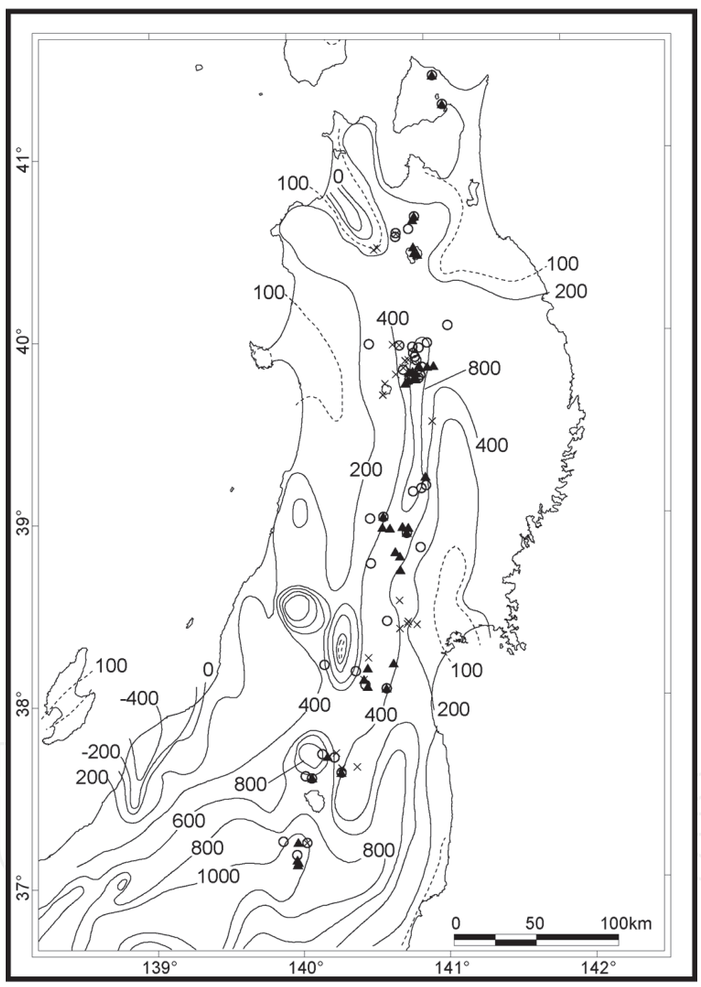

Fig. 7. Distribution of volcanic centers for each stage of Quaternary volcanism (Cross : Stage 1 , Open circle : Stage 2a , Solid triangle : Stage 2b) and amounts of Quaternary uplift and subsidence. Contour interval of uplift/subsidence is 200 m for solid line, and 100 m for broken line.

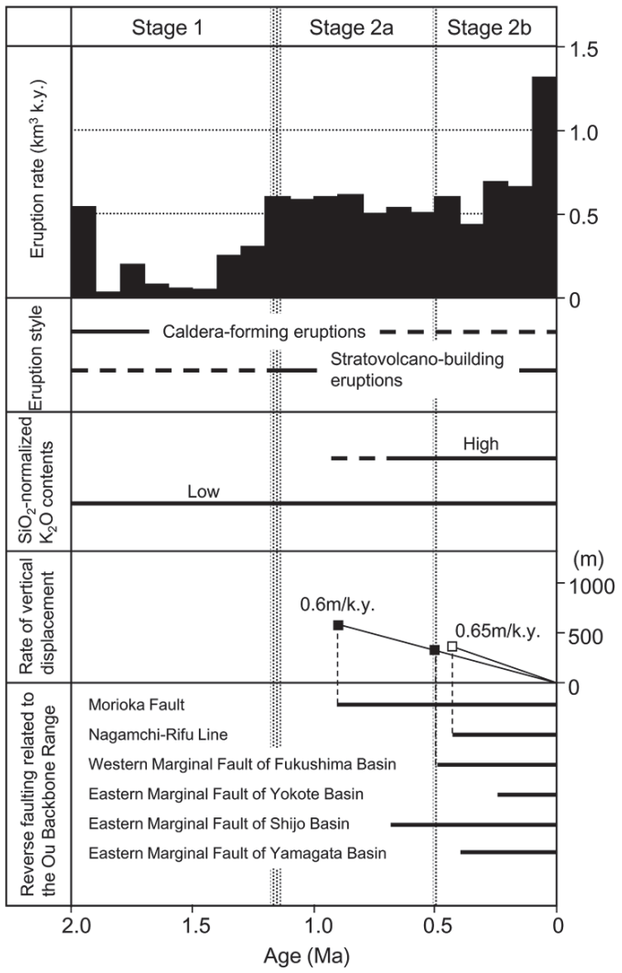

Fig. 8. Summary of volcanism and tectonism since 2.0 Ma along the volcanic front in the Northeast Japan arc.

5. Discussion

In view of the temporal and spatial connections between volcanism and tectonism discussed above, notable changes in eruption style and magma discharge rate occurred around 1.2 Ma. Generally, the crustal stress regime is thought to reflect the eruption style. Caldera formation suggests a tectonic environment facilitating the emplacement of shallow, large-scale felsic magma reservoirs. Therefore, Yoshida et al. (2001) suggested that an intermediate stress field allowing the alternation of weakly compressive and tensile fields is more favourable than a strongly tensile field to develop such a tectonic environment. Similarly, Takahashi (1995) pointed out that the accumulation of a large amount of felsic magma requires a relatively stable tectonic environment with a low crustal strain. In contrast, in stage 2, the crustal stress along the volcanic front is inferred to been changed to a strong compressive stress field with a high crustal strain rate which is favourable for stratovolcano-building volcanism. Although compressive components in the crustal stresses have gradually increased toward the fore-arc side since the Pliocene, the patterns of crustal stress are concordant with the eruption styles in stage 1 and stage 2.

However, it seems to be difficult to interpret a significant increase in erupted magma volume since ca. 1.2 Ma on account of compressional stress regime in fore-arc side. Because, in compressional settings, it is considered that magma cannot ascend so easily, for the reason of magma expanding along horizontal fractures perpendicular to the least principal stress (σ_3) equal to vertical stress (σ_v) (Hubbert and Willis, 1957). For this apparent contradiction, one of the plausible interpretation for this contradiction may be the increase in magma generation in the wedge mantle. Numerical simulations considering fluid migration and melting in the mantle wedge above a subducting plate indicate that melt production rates increase with increasing convergence rate (Cagnioncle et al., 2007). In the Cascade volcanic arc, the convergence rate of the Juan de Fuca plate to the North American plate is thought to control the change in eruption rate (Priest, 1990). Therefore, despite the overall compressive setting along the NE Japan arc, the increase of magma erupted could be interpreted to be due to the product of partial melting in the wedge by significantly faster subducting Pacific slab.

In addition, it is necessary to examine the effect of local crustal stress along the volcanic front on volcanism in stage 2. Local changes in crustal stress are attributable to: 1) the heterogeneity of differential stress caused by thermal structures (Watanabe et al., 1999); 2) a change in crustal stress near the faults caused by faulting (Yoshioka and Suzuki, 1997); and 3) the gravitational instability generated in uplifted mountain blocks (Moriya 1983; Molnar 1986).

5.1 Heterogeneity of differential stress caused by thermal structures

Watanabe et al. (1999) pointed out that the heat spreading from magma reservoirs can produce a horizontal stress heterogeneity which could be lowered locally around the reservoirs, so that the regional crustal stress could be maintained at some distance from the reservoir. In fact, a S-wave reflection horizon correlative to a magma reservoir at a depth of 7 to 12 km below the Kiso-Ontake Volcano has been recognized (Inamori et al., 1992). The focal mechanisms of swarm earthquakes generated near this horizon indicate that σ_{Hmax} is always equal to σ_1, whereas the vertical stress (σ_v) is unstable switching from σ_2 to σ_3 (Hori et al., 1982). A stress field with $\sigma_v = \sigma_2$ could lead to the intrusion of a dike and permit vertical migration of magma. Thus, even though the regional stress field is compressive, magma could still ascend if the adjacent differential stress is lowered by the heat spreading from magma itself. Moreover, it is probable that dikes, conduits for magma are combined with horizontal sheets to form a complicated plexus as indicated by Takahashi (1994). Thus, the local lowering of differential stress by thermal effects is thought to be a factor in magma ascent.

5.2 Change in crustal stress near the faults caused by faulting

It has been noted that the crustal stress around faults changes before and after faulting. According to Yoshioka and Suzuki (1997), when a dislocation is generated by a fault, a reverse fault type of stress field with $\sigma_v = \sigma_3$ develops on upward and downward extensions of the fault plane, whilst a normal fault type of stress field with $\sigma_v = \sigma_1$ occurs immediately above and below it. As mentioned above, active fault systems exist that are believed to reach the lower crust beneath the volcanic front and contribute to the uplifting of the Ou Backbone Range. Dislocations along these faults give rise to a normal fault type of stress field that facilitates the ascent of magma around faults. Therefore, it is probable that the faulting activated all over the Ou Backbone Range since 0.5 Ma resulted in the concentration of

volcanic centers in the area between western and eastern marginal active faults during stage 2b.

5.3 Gravitational instability generated in the uplifted mountain block

The uplift of the volcanic front is believed to have been accelerated by the activation of faults all over the Ou Backbone Range since 0.5 Ma. The uplift-related gravitational instability in the mountain blocks in turn is expected to have generated a tensile stress field normal to the elongation of the mountain range (Moriya 1983; Molnar 1986). Based on the fact that the focal mechanism of earthquakes below the volcanoes on the uplifted mountains differs at depth from one another, Takahashi (1994) estimated that the local tensile stress field generated by the gravitational instability may extend down to several km below the mountain top. These facts show that the more severely uplifted areas form a favourable environment for magma ascent due to the local tensile stress field, and provide a reasonable explanation for the increase in eruptive volume and the concentration of volcanic centers in such uplifted areas in stage 2b (Fig. 7). Furthermore, the N-S alignment of volcanic centers in stage 2b might reflect the E-W tensile stress field generated by gravitational instability.
Thus, the faulting and uplifting have presumably generated local lowering of differential stress or the tensile stress field along the volcanic front during stage 2, which in turn affected the amount of magma erupted and the alignment of volcanic centers. In the areas (e.g. the Hakkoda-Towada V.R, the Kurikoma-Onikobe V.R.) where volcanism associated with large-scale felsic pyroclastic flows occurred in stage 2b, a tectonic environment characterized by weak compression and a low crustal strain might have prevailed despite the lack of active faults and uplift.

6. Conclusions

From a compilation and analysis of stratigraphy, radiometric age and eruptive magma volume data for 139 volcanic events along the volcanic front, notable changes in eruption style, magma compositions, variation in eruptive volume, and distribution of volcanic centers can be recognized around 1.2 Ma. Before ca. 1.2, felsic caldera-forming volcanism are thought to occur in regions of neutral stress regime with low crustal strain rate. From ca. 1.2 Ma to the present-day, the crustal stress regime seems to have changed to compression yielding the formation of stratovolcanoes all the volcanic front. It has become apparent that stratovolcanoes lie along major thrust faults associated with uplift of the Ou Backbone Range since the Middle Pleistocene. Although it is widely assumed that magma cannot rise so easily in compressional setting, the increase of erupted magma volume since ca. 1.2 Ma may have been caused by an increase in subduction rate of the Pacific plate between 5 and 2 Ma. In addition, the lowering of differential stress by thermal effects is also thought to facilitate the ascent of magma. On the other hand, the distribution of volcanic centers formed since 0.5 Ma, controlled mostly by the local extensional stress regime in the upper crust, was locally influenced by fault dislocations and gravitational instability.

7. Acknowledgment

The author thanks Drs. R. I. Tilling, S. J. Day and S. Hayashi for many comments that helped us to improve the original manuscript, and Dr. A. J. Martin for editing this manuscript.

8. References

Acocella, V., Yoshida, T., Yamada, R. & Funiciello, F. (2008), Structural control on Late Miocene to Quaternary volcanism in the NE Honshu arc, Japan. *Tectonics*, 27, TC5008. doi:10.1029/2008TC002296.

Aramaki, S. & Ui, T. (1978). *List of geodynamic parameter of Quaternary volcanoes of Japan, Mariana, Kurile and Kamchatka.*, Geodynamics Project 78-2., Japan.

Awata, Y. & Kakimi, T. (1985). Quaternary tectonics and damaging earthquakes in northeast Honshu, Japan. *Earthquake Predict. Res.*, 3, 231-251.

Ban, M., Oba, Y., Ishikawa, K. & Takaoka, N. (1992). K-Ar dating of Mutsu-Hiuchidake, Osoreyama, Nanashigure, and Aoso volcanoes of the Aoso-Osore volcanic zone - The formation of the present volcanic zonation of the Northeast Japan arc -. *J Mineral. Petrol. Econ. Geol.*, 87, 39-49.

Cagnioncle, A.-M., Parmentier, E. M. & Elkins-Tanton, L. T. (2007). Effect of solid flow above a subducting slab on water distribution and melting at convergent plate boundaries. *J. Geophys. Res.*, 112, B09402, doi:10.1029/2007JB004934.

Committee for Catalogue of Quaternary Volcanoes in Japan (1999). *Catalogue of Quaternary Volcanoes in Japan*, Volcanol. Soc. Jpn., Tokyo, Japan.

Cox, A., & Engebretson, D. (1985). Change in motion of Pacific Plate at 5 Myr BP. *Nature*, 313, 472-475.

Hasegawa, A., Nakajima, J., Umino, N. & Miura S. (2005). Deep structure of the northeastern Japan arc and its implications for crustal deformationand shallow seismic activity. *Tectonophys.*, 403, 59-75.

Hori, S., Aoki, H. & Ooida, T. (1982). Focal mechanisms of the earthquake swarm southeast of Mt. Ontake, central Honshu, Japan. *Zisin*, 35, 161-169.

Hubbert, M. K. & Willis, D. G. (1957). Mechanics of hydraulic fracturing, In: *Structural Geology*, M. K. Hubbert, (Ed.), 175-190, Macmillan, New York.

Jolivet, L., Tamaki, K. & Fournier, M. (1994). Japan Sea, opening history and mechanism: A synthesis. *J. Geophys. Res.*, 99 (B11), 22237-22259.

Kimura, J. & Yoshida, T. (2006). Contributions of slab fluid, mantle wedge and crust to the origin of Quaternary lavas in the NE Japan arc. *J. Petrol.*, 47, 2185-2232.

Martin, A. J., Umeda, K., Connor, C. B., Weller, J. N., Zhao, D. & Takahashi, M. (2004). Modeling long-term volcanic hazards through Bayesian inference: An example from the Tohoku volcanic arc, Japan. *J. Geophys. Res.*, 109, B10208, doi: 10.1029/2004JB003201.

Molnar, P. (1986). The structure of mountain ranges. *Sci .Am.*, 255, 64-73.

Nakagawa, M., Shimotori, H. & Yoshida, T. (1988). Across-arc compositional variation of the Quaternary basaltic rocks from the Northeast Japan arc. *J. Miner. Petrol. Econ. Geol.*, 83, 9-25.

Nakamura, K. (1983). Possible nascent trench along the eastern Japan Sea as the convergent boundary between Eurasian and North American plates. *Bull. Earthq. Res. Inst., Univ. Tokyo*, 58, 711–722.

Nakata, T. & Imaizumi, T. (2002). *Digital active fault map of Japan (DVD-ROM)*, Univ. Tokyo Press, ISBN 978-413-0607-40-7, Tokyo, Japan.

Notsu, K. (1983). Strontium isotope composition in volcanic rocks from the Northeast Japan arc. *J. Volcanol. Geotherm. Res.*, 18, 531-548.

Ono, K., Soya, T. & Mimura, K. (1981). *Volcanoes of Japan, 1:2,000,000 map series, no.11, 2nd ed.*, Geol. Surv. Jpn., Tsukuba, Japan.

Otsuki, K. (1990). Neogene tectonic stress fields of northeast Honshu arc and implications for plate boundary conditions. *Tectonophys.*, 181, 151-164.

Otsuki, K., Nakata, T. & Imaizumi, T. (1977). Quaternary crustal movements and block model in the southeastern region of the Northeast Japan. *Earth Sci.*, 31, 1-14.

Pollitz, F. F. (1986). Pliocene change in Pacific Plate motion. *Nature*, 320, 738-741.

Priest, G. (1990). Volcanic and Tectonic Evolution of the Cascade Volcanic Arc, Central Oregon. *J. Geophys. Res.*, 95 (B12), 19583-19599.

Research Group for Quaternary Tectonic Map. (1968). Quaternary Tectonic Map of Japan. *Quaternary Res.*, 7, 182-187.

Sakuyama, M. & Nesbitt, R. W. (1986). Geochemistry of the Quaternary volcanic rocks of the Northeast Japan arc. *J. Volcanol. Geotherm. Res.*, 29, 413-450.

Sato, H. (1994). The relationship between late Cenozoic tectonic events and stress field and basin development in northeast Japan. *J. Geophys. Res.*, 99, (B11), 22261-22274.

Taira, A. (2001). Tectonic evolution of the Japaneses island arc system. *Annu. Rev. Earth Planet. Sci.* , 29, 109-134.

Takahashi, M. (1994). Structure of polygenetic volcano and its relation to crustal stress field 2. P-type • O-type volcano. *Bull Volcanol Soc Jpn.*, 39, 207-218.

Takahashi, M. (1995). Large-volume felsic volcanism and crustal strain rate. *Bull Volcanol Soc Jpn.*, 40, 33-42.

Tamaki, K. & Honza, E. (1985). Incipient subductionand obduction along the eastern margin of Japan Sea. *Tectonophysics*, 119, 381-406.

Tamura, Y., Tatsumi, Y., Zhao, D. P., Kido, Y., & Shukuno, H. (2002). Hot fingers in the mantle wedge: new insights into magma genesis in subduction zones. *Earth. Planet. Sci. Lett.*, 197, 105-116.

Tatsumi, Y. & Eggins, S. (1995). *Subduction zone magmatism*, Blackwell, ISBN 978-086-5423-61-9, Cambridge.

Umeda, K., Hayashi, S., Ban, M., Sasaki, M., Oba, T., & Akaishi, K. (1999). Sequence of volcanism and tectonics during the last 2.0 million years along the volcanic front in Tohoku district, NE Japan. *Bull. Volcanol. Soc. Jpn.*, 44, 233-249.

Watanabe, T., Koyaguchi, T. & Seno, T. (1999). Tectonic stress controls on ascent and emplacement of magmas. *J. Volcanol. Geotherm. Res.*, 91, 65-78.

Yoshioka, S. & Suzuki, H. (1997). Effects of three-dimensional Inhomogeneous viscoelastic structures on quasi-static strain and stress fields associated with dislocation on a rectangular fault. *Zisin*, 50, 277-289.

Yoshida, T. (2001). The evolution of arc magmatism in the NE Honshu arc, Japan. *Tohoku Geophys. J.*, 36, 131-149.

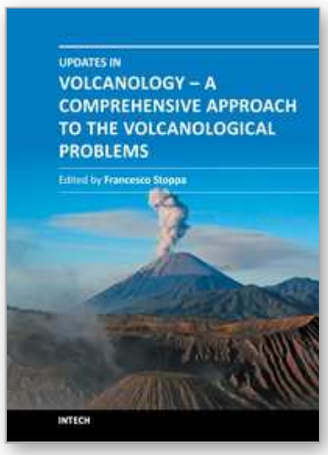

Updates in Volcanology - A Comprehensive Approach to Volcanological Problems

Edited by Prof. Francesco Stoppa

ISBN 978-953-307-434-4
Hard cover, 242 pages
Publisher InTech
Published online 13, January, 2012
Published in print edition January, 2012

This book ranges from the geologic-petrologic description of world-wide major volcanic fields unfamiliar to international literature, to the discussion and interpretation of the results in light of geophysical techniques. It focuses on several situations that represent large-scale volcanism on Earth, related both with intra-plate or active margins. Many large volcanic complexes of Easter countries are presented, including Japan, Siberian Russia, and Mongolia. A detailed account of the European volcanic province of the Pannonia basin and Central-Southern Spain is given. Southern hemisphere areas of Antarctica and Polynesia are considered as well. The chapters are very informative for those who wish for a guide to visiting, or are curious about main characteristics of the above volcanic areas, some of which are remote and not easily accessible.

How to reference

In order to correctly reference this scholarly work, feel free to copy and paste the following:

Koji Umeda and Masao Ban (2012). Quaternary Volcanism Along the Volcanic Front in Northeast Japan, Updates in Volcanology - A Comprehensive Approach to Volcanological Problems, Prof. Francesco Stoppa (Ed.), ISBN: 978-953-307-434-4, InTech, Available from: http://www.intechopen.com/books/updates-in-volcanology-a-comprehensive-approach-to-volcanological-problems/quaternary-volcanism-along-the-volcanic-front-in-northeast-japan

INTECH
open science | open minds

InTech Europe
University Campus STeP Ri
Slavka Krautzeka 83/A
51000 Rijeka, Croatia
Phone: +385 (51) 770 447
Fax: +385 (51) 686 166
www.intechopen.com

InTech China
Unit 405, Office Block, Hotel Equatorial Shanghai
No.65, Yan An Road (West), Shanghai, 200040, China
中国上海市延安西路65号上海国际贵都大饭店办公楼405单元
Phone: +86-21-62489820
Fax: +86-21-62489821

IntechOpen